

Full Length Research Paper

Phloretin induced apoptosis of human hepatoma cells SMMC-7721 and its correlative biological mechanisms

Hui Wang^{1,2#}, Dianjun Wang^{3#}, Yabin Pu¹, Dengkui Pan⁴, Weijun Guan^{1*} and Yuehui Ma^{1*}

¹Institute of Animal Science, Chinese Academy of Agricultural Sciences, Beijing 100193, China.

²College of Wildlife Resources, Northeast Forestry University, Harbin 150040, China.

³Department of Pathology, People's Liberation Army General Hospital, Beijing 100853, China.

⁴College of Science and Art, Shanxi Agricultural University, Shanxi 030801, China.

Accepted 8 February, 2012

In order to investigate the proliferative and apoptotic effects of phloretin on human hepatoma cell line SMMC-7721 and to explore the mechanisms of phloretin induced apoptosis, this research is set to observed morphological alterations with phase contrast and confocal microscopy, performed MTT assay, and detected apoptotic rates, cell cycle progression, mitochondrial trans-membrane potential and intracellular calcium homeostasis. The results suggested that typical apoptotic morphological alterations occurred after phloretin treatment. Phloretin exerts a strong inhibitory on the proliferation of SMMC-7721 cell line, and induces its apoptosis in a dosage and duration dependent manner. Cell cycle was arrested at G1 phase. Mitochondrial trans-membrane potential dropped. Calcium homeostasis was disturbed. It is concluded that phloretin can induce apoptosis of SMMC-7721 via arresting cell cycle progression, reducing mitochondrial trans-membrane potential and disturbing intracellular calcium homeostasis.

Key words: Apoptosis, phloretin, human hepatoma cells, SMMC-7721 cells.

INTRODUCTION

One of the most important mechanisms underlying tumorigenesis is uncontrolled proliferation and apoptosis. Consequently, the crux of tumor therapy is to inhibit cell division and induce apoptosis. Apoptosis occurs through activation of a cell suicide process regulated by many different intracellular and extracellular events. Apoptosis is governed by several genes, some of which are mutated or dysfunctionally regulated in various types of human tumors (Brown and Attardi, 2005). Apoptosis, as programmed cell death, is the most well-defined type of cell death pathway, both morphologically and biochemically. It is characterized by membrane blebbing, cytoplasmic shrinkage and reduction of cellular volume (pyknosis), condensation of the chromatin, and

fragmentation of the nucleus (karyorrhexis), all of which ultimately lead to formation of apoptotic bodies, a prominent morphological feature of apoptotic cell death (Kroemer et al., 2005).

Induced apoptosis of tumor cells provides a new strategy and was believed to hold profound significance for prevention and cure of neoplastic transformation. Cancer is a prevailing lethal pathology, and commonly used therapies of hepatoma can hardly achieve satisfactory results. Traditional Chinese medicine, the essence accumulated throughout centuries, attracts more and more attention owing to its remarkable curative effects on cancer. Drug induced apoptosis of malignant cells is presumably a promising tumor therapeutic strategy and emerging evidence is supporting its effectiveness against hepatoma as well as other cancers.

Phloretin, a natural active compound, belongs to flavonoids, exists in sap of apple, pear and other fruits and vegetables. Phloretin has been studied as a possible penetration enhancer for skin-based drug delivery (Auner et al., 2003), attenuates inflammation by antagonizing

*Corresponding author. E-mail: Yuehui_Ma@hotmail.com; weijunguan301@gmail.com.

#These authors contributed equally to this article.

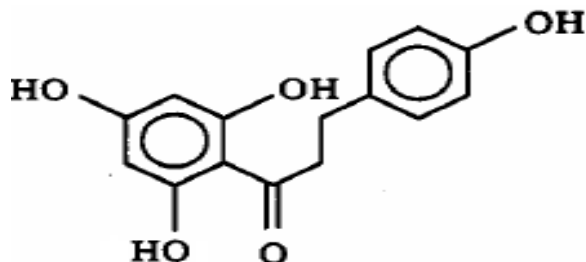


Figure 1. The molecular structure of phloretin (chemical formula: $C_{15}H_{14}O_5$, molecular weight: 274.27).

prostaglandins (Blazso and Gabor, 1995), protects the skin from UV light-induced photodamage (Oresajo, 2008), and is currently evaluated as a chemopreventive agent for cancer treatment. It can serve the purposes of anti-oxidation, antitumor, anti-diabetes, antibiosis and para-hormone under physiological context (Chih-Hsiung, 2009; He, 2007; Yoon and Liu, 2007). Besides its potent antioxidant property, phloretin is known to be a competitive inhibitor of sodium *D*-glucose cotransporter (Raja et al., 2003). Phloretin exert anti-inflammatory effect through suppressing macrophage function.

Phloretin, because of its effects on cell proliferation disorders, is one promising anti-mutagenic factors that can be used for hepatoma treatment and other tumors, and thus is a potential chemotherapeutic agent. There are 4 hydroxyls (-OH) in its chemical structure, which can well inhibit the trans-membrane transport of saccharide, leading to apoptosis of malignant cells (Figure 1). In many studies, phloretin was showed to induce apoptosis of tumor cells via diverse path ways, such as inhibition of glucose transportation, stimulation of estrogen receptor or mitochondrial pathways (Blobel and Orkin, 1996), and it has long been known as non-specific PKC inhibitor (Gschwendt et al., 1984), can inhibit cell proliferation and induce apoptosis via PKC pathway (Jarvis et al., 1994). Phloretin also inhibits the growth of bladder cancer and rat mammary adenocarcinoma cells *in vivo* (Nelson and Falk, 1993).

In elucidating the therapeutic values of phloretin, this research investigated its apoptotic effects and mechanism on human hepatoma cells.

MATERIALS AND METHODS

Human hepatoma cells SMMC-7721 was purchased from Peking Union Medical College. Phloretin was purchased from Sigma Inc. Dulbecco's modified Eagle's medium (DMEM) and fetal bovine serum (FBS) was purchased from Gibco. Annexin V-FITC Apoptosis Detection Kit I was purchased from BD corporation.

Cell culture

The cells were cultured in DMEM medium containing 10% FBS in a

37°C incubator with 5% CO_2 (Guan, 2005; Zhou, et al 2004). The medium was refreshed when it became yellow. Cells were dissociated when they reached 80 to 90% confluence and were sub-cultured into sterilized flasks at the ratio of 1:2 or 1:3.

Growth dynamics

Following the method of Gu et al. (2006) and Kong et al. (2007), cells at the concentration of 2.0×10^4 cells/ml were plated into 24-well micro plates. Data on cell growth and density were calculated and recorded each day until plateau phase; three wells were counted each time. The growth curve was then plotted and the population doubling time (PDT) was calculated according to this curve.

Drug solution preparation and treatment

Phloretin was dissolved with Dimethyl sulfoxide (DMSO), diluted with DMEM medium, filtered for sterilization, aliquoted.

It should be diluted to the required concentration with DMEM medium prior to treatment, and the final concentration of DMSO should be 0.05% in experiments, for control specimens, the same volume of 0.05% DMSO without phloretin was added. The experimental cells were logarithmic phase. After treatment with DMEM medium containing phloretin or DMSO, they were cultured to the scheduled time.

Morphological observation

Observation by inverted phase contrast microscope

2 ml suspension was plated on each well of 6-well micro plates at the concentration of 2.0×10^5 cells/well. Cells in logarithmic phase were treated with phloretin-containing complete DMEM medium for 24 h. Morphological alterations were observed and photographed using inverted phase contrast microscope.

Fluorescent observation using confocal microscopy

To visualize the morphological alterations of apoptotic nuclei, acridine orange (AO) and ethidium bromide (EB) fluorescent staining of phloretin treated cells was performed. Cells were treated by phloretin for 24 h. Cell suspension was harvested from each well, and stained with AO, EB solution (both 2 mg/ml in ethanol) of 6 μ l, and gently mixed. Incubated at room temperature in the dark for 5 min, the samples were then observed using confocal microscopy (Nikon TE-2000-E, Japan) immediately.

Observation by transmission electron microscopy

The cells of controls and experimental samples were collected, and fixed with 2.5% (m/v) glutaraldehyde, then washed with 0.1 mol/L phosphate buffered and subjected to serial dehydration with 30, 50, 70, 80, 90 and 100% acetone (v/v). The samples were embedded with epoxy resin (SPURR) for polymerization, then slice thin slices with ultramicrotome (LEICAUC6i), Uranyl acetate and lead citrate for double staining. The samples were observed using transmission electron microscopy (JEM-1230).

MTT colorimetric assay

The 3-(4, 5-Dimethylthiazol-2-yl)-2,5-diphenyltetrazolium bromide

(MTT) assay was used to evaluate cytotoxicity as described by Ho et al. (2005). Cell suspension of 200 μ l was placed on each well of 96-well micro plates at the concentration of 1.0×10^5 cells/well. Cells in logarithmic growth phase, with phloretin containing complete DMEM media and corresponding controls were set simultaneously. 6 replicates were prepared for each treatment and cultured until 12, 24, 36 and 48 h. After the addition of MTT 20 μ l (5 mg/ml phosphate buffered saline (PBS)) each well, the cells were cultured for another 4 h. The supernatant was discarded. After the addition of 200 μ l DMSO in each well, the samples were incubated in the dark for 30 min, and then swirled for mixing. Absorbance A at 490 nm was measured using enzymatic reader. Experiments were repeated three times.

Annexin V-FITC/PI double-labeling

The detection of apoptosis using annexin V-FITC/propidium iodide (PI) staining was performed as described previously (Cetindere et al., 2010). The cells of controls and experimental samples were collected and adjusted to the concentration of $(1-5) \times 10^5$ cells/ml in binding buffer. For each sample, 100 μ l cell suspensions was stained with 5 μ l fluorescein isothiocyanate (FITC) and 5 μ l PI and incubated at room temperature in the dark for 25 to 30 min. After the addition of 400 μ l binding buffer each sample, and then detected with flow cytometer (FCM) (BD FACSCalibur, USA) within 1 h.

Cell cycle progression

The cell cycle stages were measured by FCM as previously described (Ho et al., 2005). The cells of controls and experimental samples were collected and adjusted to the concentration of 1.0×10^6 cells/ml, and then spun at 1200 g, 4°C for 10 min. With supernatant discarded, they were washed twice with pre-cooling of PBS, re-suspended in ice-cold 70% ethanol (v/v), and kept at 4°C overnight. Pelleted and washed twice with PBS, the samples were stained with PI solution (PI 0.05 mg/ml, RNase 0.02 mg/ml, NaCl 0.585 g/ml, sodium citrate 1 mg/ml, pH 7.2-7.6) at 4°C for 30 min in the dark, and then detected with FCM (BD FACSCalibur, USA) immediately.

Mitochondrial transmembrane potential

Mitochondrial trans-membrane potential was determined as described previously (Yang et al, 2006; Zhang et al., 2006). The cells of controls and experimental samples were collected and adjusted to the concentration of 1.0×10^6 cells/ml, and then spun at 1200 g, 4°C for 10 min. With supernatant discarded, they were washed twice with pre-warmed PBS. After the addition of JC-1 working solution (5 μ g/ml, 0.5 ml/sample), the cells were incubated at 37°C in the dark for 10 to 15 min, and then were washed twice with pre-warmed PBS. After centrifugation at 1200 g, 4°C for 10 min, the supernatant was discarded. Each sample was re-suspended with 0.5 ml PBS, and then detected with FCM (BD FACSCalibur, USA) immediately.

Intracellular calcium homeostasis

The intracellular Ca^{2+} release was assessed by staining with Ca^{2+} -sensitive dye Fluo3-AM (Adachi, 2008). The cells of controls and experimental samples were collected and adjusted to the concentration of $(1-2) \times 10^6$ cells/ml. Fluo-3/AM (Invitrogen, USA) was added to each sample to reach a final concentration of 5-10 μ mol/L. Incubated at 37°C, 5% CO_2 in the dark for 30 to 60 min, the samples were oscillated several times gently. Prepare negative

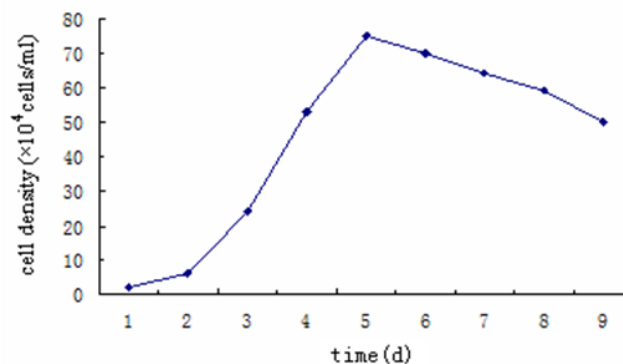


Figure 2. Growth Curve of SMMC-7721 Cells.

controls (without Fluo-3/Am) for reference. The cells were centrifuged at 1200 g, 4°C for 5 min, and washed twice with calcium-free PBS buffer, in order to remove the excessive dye. Each sample was resuspended in 0.5 ml calcium-free PBS, and then detected with FCM (BD FACSCalibur, USA) immediately.

Statistical analysis

Cytotoxicity data, apoptotic rates and cell cycle data were analyzed using the GLM procedure in Statistical Analysis System (SAS Inc., Cary, NC, USA) and compared with a multiple comparison test (DUNCAN). A value of $P < 0.05$ and $P < 0.01$ was thought of as statistically significant.

RESULTS

Growth dynamics

The growth curve of SMMC-7721 cells displayed an obvious "S" shape, and the PDT was proximately 24 h. The cells were in the latent phase in days 1 and 2, and then entered logarithmic phase in days 2 to 5. The concentration reached its peak on day 5, and then the cells entered the plateau phase in day 6, followed by an overall degeneration thenceforth (Figure 2).

Morphological observation

Observation using inverted phase contrast microscope

Under normal circumstances, the adherent cells were elliptical shaped. In logarithmic phase, the passage cells will gradually adhere and grow. The cells of the control showed that cells were closely arranged with uniform size, as well as good vitality and refractivity (Figure 3A). The phloretin treated cells displayed atrophy and vacuoles (Figure 3B), shrinkage, cell number decrease, and cell fragmentation took place (Figure 3C), with blurred contour, the declined in cells connection, and

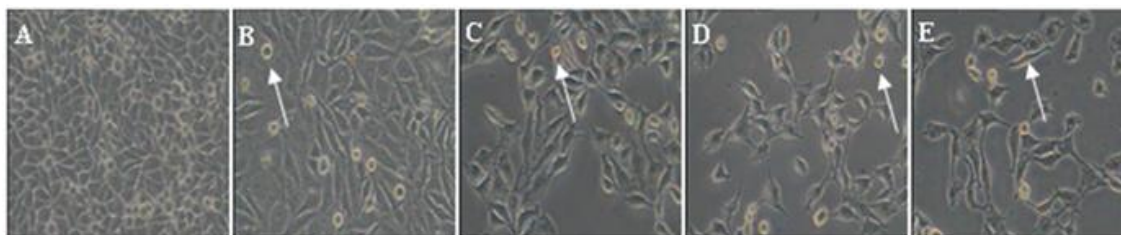


Figure 3. Morphological observation of SMMC-7721 cells by inverted phase contrast microscope. Morphology of SMMC-7721 cells at 24 h after treatment with phloretin (100 \times). (A) control; and SMMC-7721 cells treated with phloretin of (B) 20 mg/L;(C) 40 mg/L;(D) 80 mg/L and (E) 160 mg/L. apoptotic cells are marked with arrows.

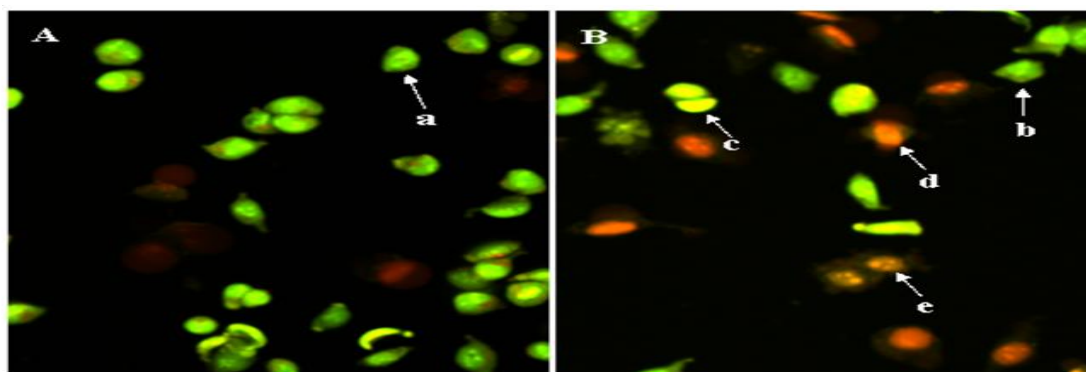


Figure 4. Morphological observation of SMMC-7721 cells using AO/EB double staining by confocal microscopy. Morphology of SMMC-7721 cells at 24 h after treatment with phloretin. Scale bars=50 μ m. (A) control; and SMMC-7721 cells treated with phloretin of (B) 80 mg/L; Arrow a and b, normal cells. Arrow c, viable apoptotic cells. Arrow d and e, non-viable apoptotic cells.

even lysed into small pieces. Apoptotic cells detached from adjacent normal cells, and are obviously different in morphology (Figure 3D and E). A typical morphological feature observed during apoptosis is the reduction of cellular volume, a feature that distinguishes this form of cell death from necrosis.

Observation using confocal microscopy

AO and EB differ in permeability and fluorescence, distinguishing cells in early apoptosis and late apoptosis. Viable apoptotic cells have intact membrane which prevents EB from entering the interior of cells, possess yellow cytosol and condensed nuclei, with condensation-like or dead-like nuclear chromatin. Membrane of non-viable apoptotic cells is permeable, through which both AO and EB will enter, thus cells will display condensed nuclei and orange fluorescence (Figure 4).

Observation by transmission electron microscopy

The control group cell (Figure 5A and C), cell plasma is

homogenous and plump, cell nucleus is large and round, nucleoli is clear and regular, chromatin is Loose. Nucleus, nuclear membrane and sub-cellular structures are intact. There is a large number of microvilli on cell surface.

Cells in the experimental group (Figure 5B and D), cell plasma format vacuoles, cell nucleus is Pyknosis, smaller, Nucleolus is shrink, concentrate or even disappear. Chromatin is aggregated, marginalized and is lumpish in the inner nuclear membrane and then heterochromatin is increase. Nuclear membrane is broken down and microvilli on cell surface are reduced. Mitochondria are a major resource and target of oxidative stress, and even play a central role in “the Free Radical Theory of Aging” (Alexeyev, 2009; Cadenas, and Davies 2000).

MTT colorimetric assay

MTT assay showed that, for phloretin treated SMMC-7721 cells at 12 h, 24 h, 36 h, and 48 h, the viable cell population decreased significantly with elevated drug concentration and duration of treatment, appearing dose- and duration-dependent (Figure 6).

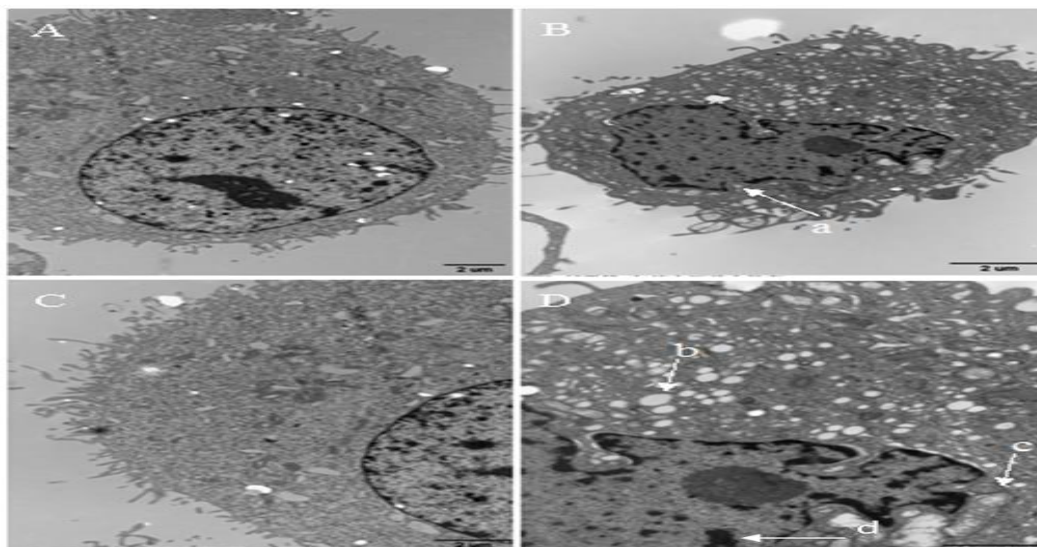


Figure 5. Subcellular observation using transmission electron microscopy. Morphology of SMMC-7721 cells at 24 h after treatment with phloretin. A, B and C Scale bars=2 μm , D Scale bars=1 μm . (A,C) control; and SMMC-7721 cells treated with phloretin of (B,D) 80 mg/L. Arrow a indicate broken nuclear membrane. Arrow b indicates vacuoles. Arrow c indicates broken mitochondrion. Arrow d indicate chromatin condensation.

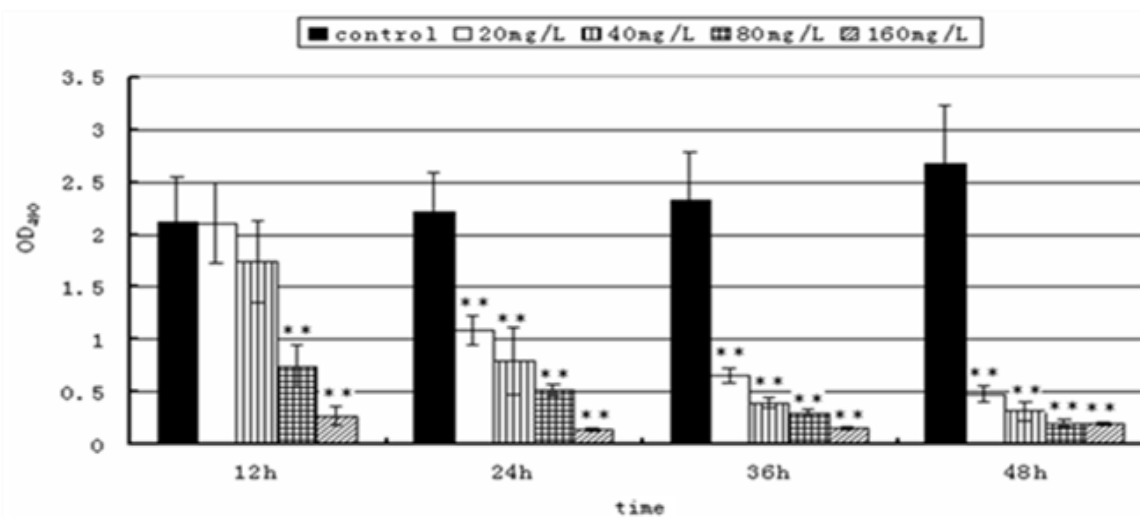


Figure 6. Cytotoxicity analysis of SMMC-7721 cells treated with phloretin, OD values reflect viable cell population size. Statistical significance to corresponding controls is marked with (*) ($P<0.05$) and (**) ($P<0.01$) ($n=8$).

Annexin V-FITC/PI double-labeling

Quantitative analysis of apoptotic effects of phloretin on SMMC-7721 cells. Apoptotic rates increased with increasing duration and concentration (Figure 7). Results interpretation: the first quadrant (FITC⁻/PI⁻), normal cells; the second quadrant (FITC⁻/PI⁺), cell debris, result from the mechanical factor for cell processing; the third quadrant (FITC⁺/PI⁺), late stage apoptotic cells and some

necrotic cells; the fourth quadrant (FITC⁺/PI⁻), early stage apoptotic cells.

Cell cycle progression

To test the mechanisms of phloretin induced SMMC-7721 cells apoptosis, cell cycle progression was analyzed by FCM. With the increasing concentration of phloretin, the

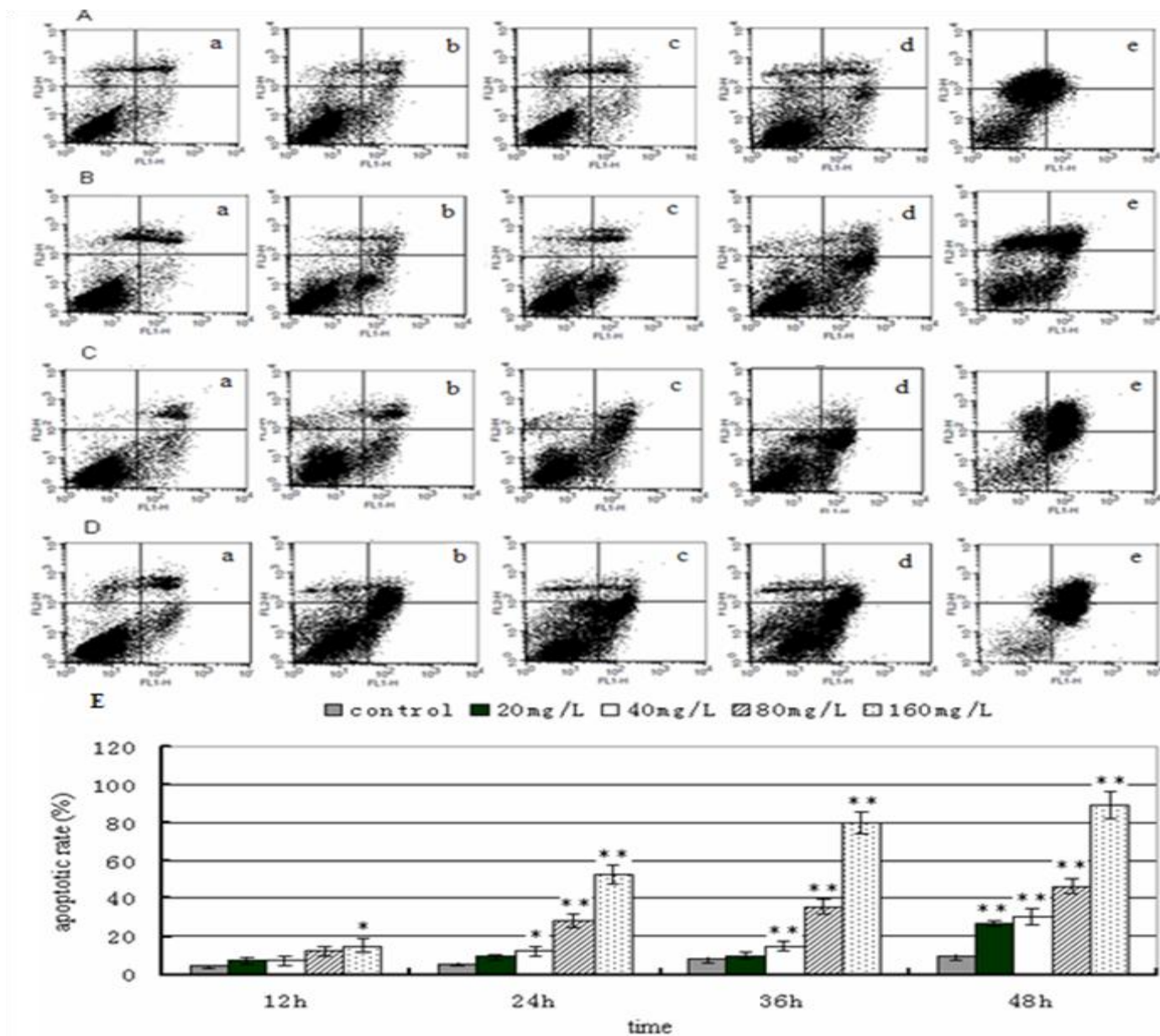


Figure 7. FACS analysis of apoptotic rates of phloretin treated SMMC-7721 cells. (A,B,C,D) The apoptotic rate of SMMC-7721 cells at 12 h, 24 h, 36 h, 48 h treatment with phloretin, respectively. a, control; and SMMC-7721 cells treated with phloretin of b, 20 mg/L; c, 40 mg/L; d, 80 mg/L and e, 160 mg/L. (E) Statistical significance to control is marked with (*) ($P < 0.05$) and (**) ($P < 0.01$) ($n = 3$).

percentage of cells increased in G1 phase, and decreased in S phase and G2 phase decreased, indicating an arrest in G1 phase, and that DNA synthesis was inhibited. The effects on cell cycle were even more significantly with elevated phloretin dose, reflecting a dose dependent correlation (Figure 8B). The percentage of apoptotic cells in hypodiploid DNA peak (sub-G1 population) was calculated by sub-G1 population / total cell cycle populations, and indicated by numbers shown in each histogram, sub-G1 population also showed dose- and time-dependent (Figure 8).

Mitochondrial trans-membrane potential

To observe the changes in mitochondrial membrane potential after treatment by phloretin, cells were stained with JC-1 and examined by FCM. JC-1 is a lipophilic, cationic dye that can selectively enter mitochondria and reversibly change color from green to red as the membrane potential increases. JC-1 dye accumulates as aggregates in the mitochondria in normal cells, which results in red fluorescence, whereas, in apoptotic or necrotic cells, JC-1 exists in monomeric form and stains

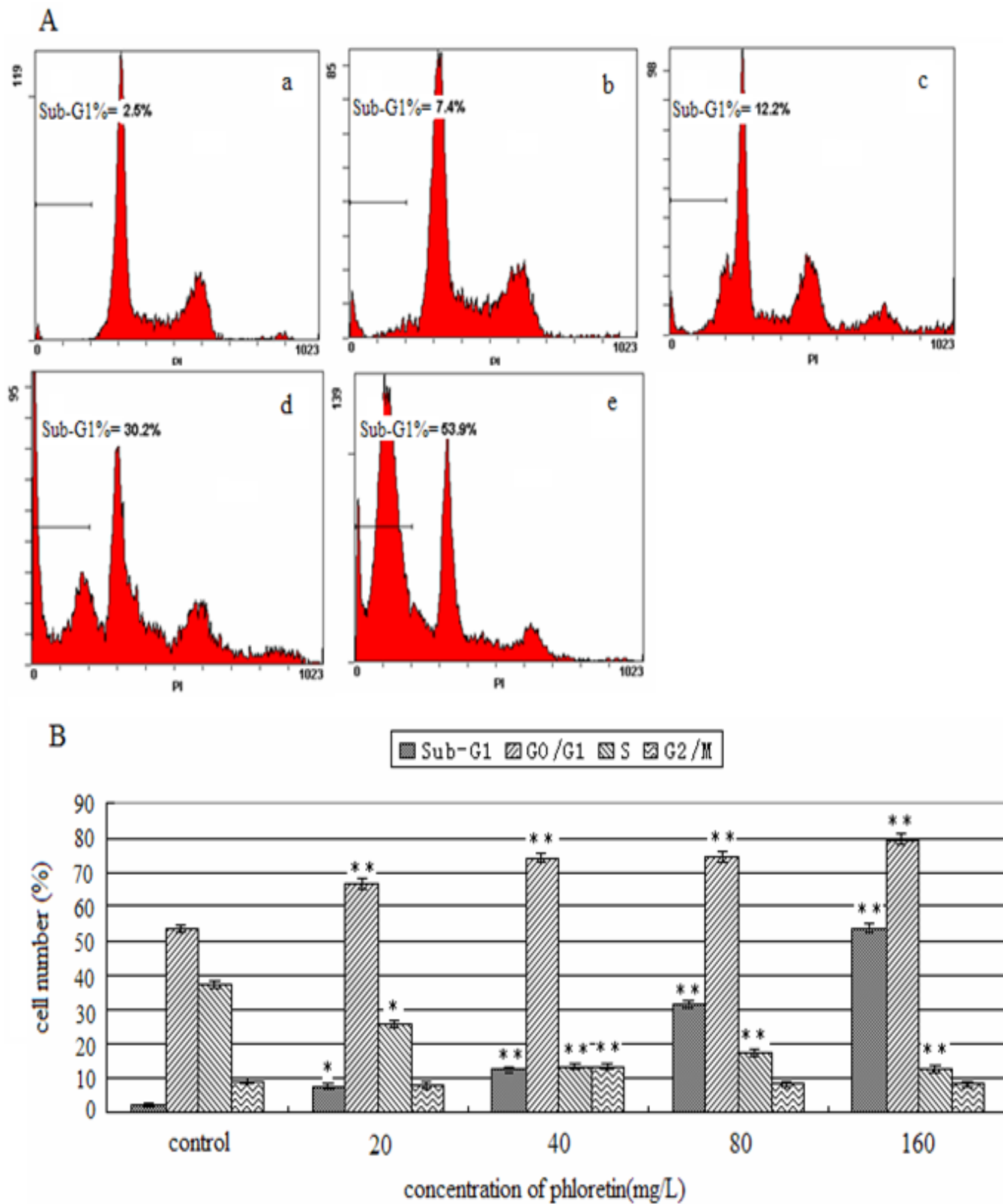


Figure 8. FACS analysis of cell cycle progression and sub-G1 content of SMMC-7721 cells at 24 h after treatment with phloretin.(A) Cell cycle distribution histograms, the percentage of apoptotic cells in hypodiploid DNA peak (sub-G1 population) was calculated by sub-G1 population/total cell cycle populations, and indicated by numbers shown in each plot. a,control; and SMMC-7721 cells treated with phloretin of b,20 mg/L;c,40 mg/L;d,80 mg/L and e,160 mg/L.(B)Statistical significance to control is marked with (*) ($P<0.05$) and (**) ($P<0.01$) (n=3).

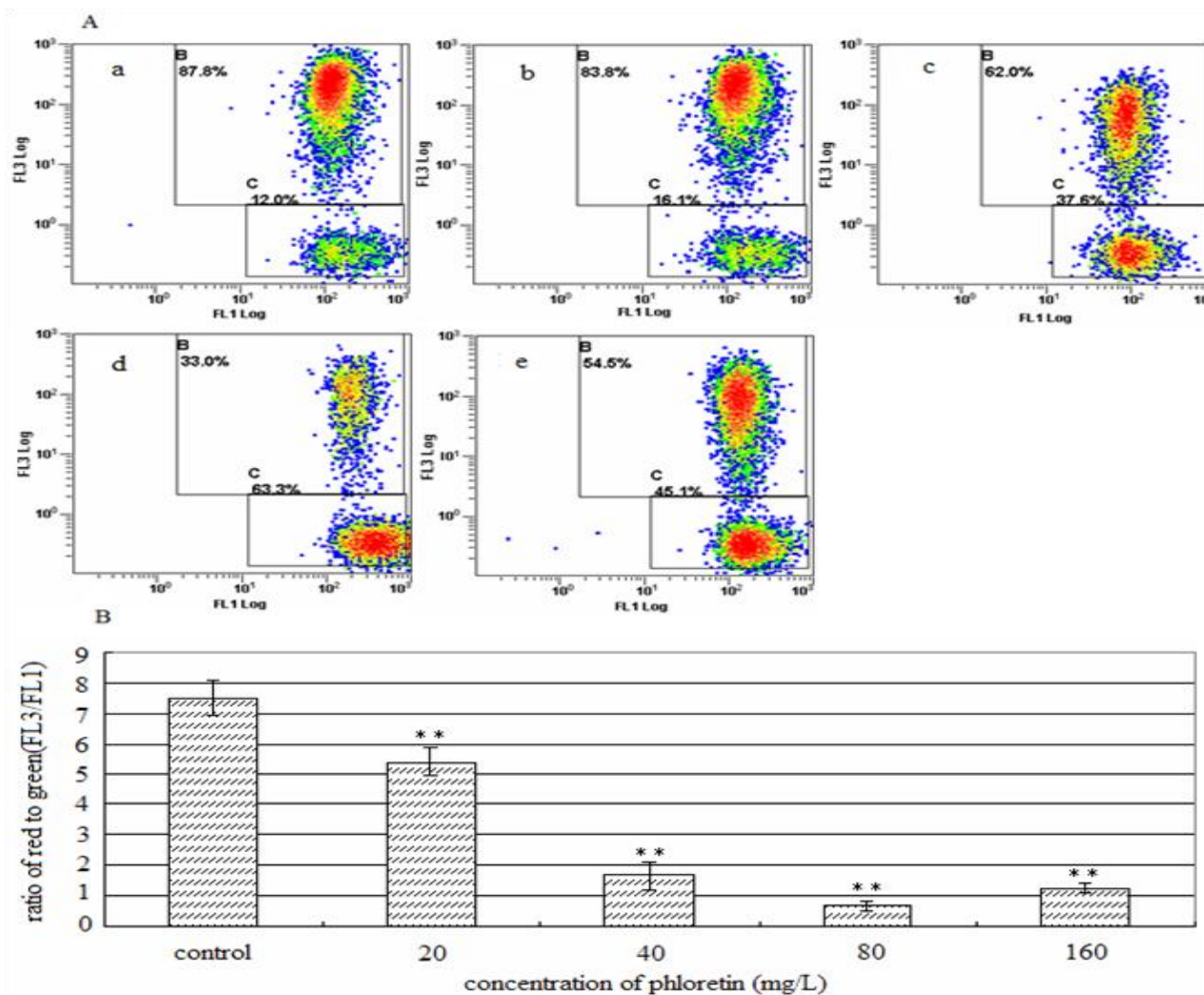


Figure 9. FACS analysis of the mitochondrial membrane potential of SMMC-7721 cells at 24 h after treatment with phloretin. (A) a, control; and SMMC-7721 cells treated with phloretin of b, 20 mg/L; c, 40 mg/L; d, 80 mg/L and e, 160 mg/L. (B) Cells were stained with JC-1 and examined by FCM. Active mitochondria with high transmembrane potential form JC-1 aggregates, which are red (FL3, 620 nm), whereas in mitochondria with low transmembrane potential, JC-1 remains in a monomeric, green form (FL1, 527 nm). The ratio of red to green (FL3/FL1) reflects the change in mitochondrial membrane potential. Statistical significance to control is marked with (*) ($P < 0.05$) and (**) ($P < 0.01$) ($n = 3$).

the cytosol green. The cells number of C gate reflects the change of mitochondrial trans-membrane potential. The increase of cells number of C gate means decrease of mitochondrial trans-membrane potential (Figure 9A). Mitochondrial trans-membrane potential significantly dropped after treatment with phloretin, displayed significant differences compared with the control (Figure 9B). Decreased mitochondrial transmembrane potential has been linked to apoptotic cell.

Intracellular calcium homeostasis

SMMC-7721 cells at 24 h after treatment with phloretin

and were subsequently labelled with the molecular probe Fluo-3/AM. The results show that peak position in the histograms reflects the intracellular Ca^{2+} concentration of phloretin treated SMMC-7721 cells (Figure 10A). The Ca^{2+} concentration of experimental samples treated with phloretin of 20, 40, 80 and 160 mg/L displayed significant differences compared with the controls. It was revealed that there is a positive correlation between Ca^{2+} release and phloretin concentration (Figure 10B).

DISCUSSION

Phloretin are polyphenols widely distributed in the plant kingdom, and they are present in fruits and vegetables

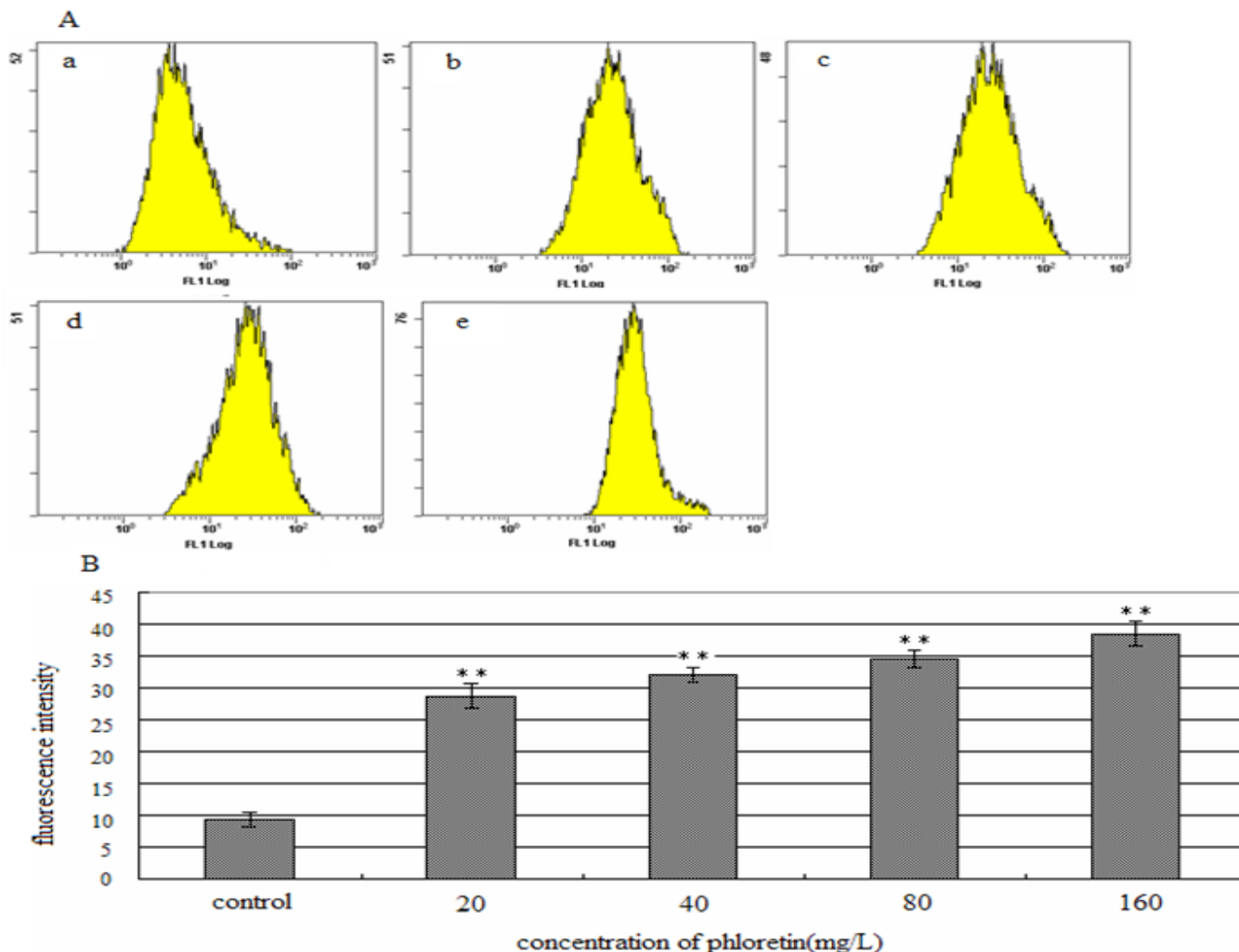


Figure 10. FACS analysis of intracellular calcium homeostasis of SMMC-7721 cells at 24 h after treatment with phloretin. (A) a, control; and SMMC-7721 cells treated with phloretin of b, 20 mg/L; c, 40 mg/L; d, 80 mg/L and e, 160 mg/L. Peak moving to the right means an increase of intracellular Ca²⁺ concentration. (B) Statistical significance to control is marked with (*) ($P < 0.05$) and (**) ($P < 0.01$) ($n = 3$).

regularly consumed by humans. Phloretin, a polyphenolic compound, have potent anti-inflammatory, anti-oxidative, and even some anticancer activities form the scientific basis for the common saying “an apple a day keeps the doctor away.”

Phloretin can inhibit tumor formation and induce apoptosis of tumor cells (So, 2006; Zhang, 2007). One study showed that 200 μM Phloretin was used to induce HepG2 cell apoptosis (Brown and Attardi, 2005), and phloretin at 30 μM protected peptide-induced plasma membrane damage in PC12 cells, while 300 μM Phloretin became toxic to the cells (Hertel et al., 1997). Using primary rat hepatocytes, previous reports demonstrated that Phloretin at 0.4 to 200 μM significantly reduced tert-butyl hydroperoxide-induced cytotoxicity (An et al., 2007), and reported that the LD₅₀ of Phloretin is 500 \pm 51 μM (Moridani et al., 2002).

Our study evaluated a wide variety of apoptotic indices, and definitely proved that a certain concentration of phloretin can inhibit the proliferation of SMMC-7721 cells and induce apoptosis, and hence have huge anti-tumor effects.

Cell cycle progression

It is generally believed that physiological or pathological apoptotic stimuli are correlated with cell cycle progression (Siegers et al., 1999). Unscheduled proliferation constitutes a key step in canceration, and an altered death to division speed would eventually lead to malignant transformation and neoplastic growth (Frantz et al., 2000). Currently considered, cell cycle arrest would induce apoptosis, and influence proliferation. Many

apoptotic signals affect apoptotic machineries as well as cell cycle progression at the same time. Therefore cell cycle analysis is one of the most important evaluations in apoptotic research. Furthermore, blocking cell cycle to induce apoptosis now serves as a new target for anticancer drugs. Structurally similar to glucose, phloretin has the molecular structure of 4-hydroxy and thus forms non-competitive inhibition with glucose transport, inhibit energy source and promote apoptosis.

One study shows that treatment of HepG2 cells with 100 and 150 μM phloretin for 24 h slightly increased the populations in G0/G1 and G2/M, respectively. In contrast, treatment of HepG2 cells with 200 μM phloretin for 24 h significantly induced HepG2 cell death, evidenced by an increase in the sub-G1 population (Chih-Hsiung et al., 2009). By cell cycle analysis after Phloretin treatment, it was found that the cells were arrested in G1 phase with decreased proportion of S and G2 phases, causing a reduction in M phase and inhibited cell division. With elevated phloretin concentration, the proportion of cells in G1 phase, hypodiploid DNA (sub-G1 population) increased and that of cells in S phase decreased. Therefore, we speculate that with the aromatic ring structure phloretin can insert into the DNA double helix, thereby preventing DNA synthesis, affecting cell cycle progression and leading to apoptosis.

Treatment with 40 mg/L phloretin increased in G2 phase proportion, whereas 80 mg/L phloretin decreased in G2 phase proportion. This is possibly due to that 40 mg/L of phloretin mainly prevents cells entering G1 phase, and then S/G2 transition, therefore leading to a temporary increase in G2 phase. With increased phloretin concentration, 160 mg/L of phloretin caused the cells number of G2 phase to reduce. It is likely that phloretin plays a role in cell cycle progression and thus exerts its effects in apoptosis. This provides an important experimental basis for future mechanism study of phloretin induced apoptosis in hepatoma cells.

Mitochondrial trans-membrane potential

Apoptosis occurs through activation of a cell suicide process regulated by many different intracellular and extracellular events. It is generally accepted that caspases play an essential role in the induction and execution of apoptosis. There are two distinct pathways leading to caspase activation and ensuing apoptosis, the death receptor pathway and the mitochondrial pathway. In the apoptotic process, many important events including are closely related with mitochondrion (Bouchier-Hayes et al., 2005), which is that mitochondrial trans-membrane potential drops (Amstrong, 2006), membrane permeability increases, mitochondrial permeability transition pore opens (Disa, and Bailly 2005; Lucken-Ardjomande, 2005), and then mitochondria of cytochrome C (Mohamad et al., 2005), apoptosis inducing factor (AIF)

(Liu et al., 1997), etc. enter the cytoplasm, starting the process of apoptosis. In the mitochondrial pathway, the release of cytochrome c from mitochondria is a crucial step in the activation of caspases. Once released to the cytosol, cytochrome c associates with apoptosis protein-activating factor-1 (Apaf-1), forming an apoptosome complex that, in the presence of ATP or dATP, is capable of activating procaspase-9. Initiator caspases, activated through either one of these two pathways, can in turn activate caspase-3 and other effector caspases responsible for dismantling of the dying cell. Therefore, biochemical and morphological changes, including cellular shrinkage, chromatin condensation and DNA fragmentation, are almost invariably involved in both pathways (Johansson et al., 2003).

The drop of mitochondrial trans-membrane potential is considered to be the first event of apoptotic signaling, which occurs before occurrence of apoptotic characteristics in nuclear. The present study of apoptotic mechanism shows that mitochondrion plays a pivotal role in the process of apoptosis. Mitochondrial trans-membrane potential will change when apoptosis happens, leading to changes in membrane permeability. Mitochondrial membrane potential, the driving force of ATP production, is decreased during apoptosis (Richter et al., 1996). ATP depletion is an important mechanism of apoptosis (Moley, 2005; Nakamura, and Wada 2000).

Phloretin is an uncoupler, which can inhibit mitochondrial oxidative phosphorylation (Jonge et al., 1983), block ATP synthesis, decrease energy generation, and hence induce apoptosis. In this study, cells labeled with JC-1 staining solution were subjected to flow cytometry detect changes in mitochondrial trans-membrane potential. It was found mitochondrial trans-membrane potential decrease in SMMC-7721 cells upon treatment with phloretin, subsequently by the possible suppression of ATP production even lead to ATP depletion and breakdown of mitochondria, activating downstream apoptotic pathways, therefore, suggesting that phloretin induced apoptosis of SMMC-7721 cells is related to mitochondrial pathway.

Intracellular calcium homeostasis

In normal cells, Ca^{2+} mainly combined with protein cistern in endoplasmic reticulum and mitochondrion. There is little dissociative Ca^{2+} , unless the receipt of external stimuli trigger its release as molecule messenger. Almost all cell responses, including contraction, exocytosis, gene expression and apoptosis, are controlled by partial or total change dissociative Ca^{2+} concentration. Research has shown that the excessive accumulation of intracellular free Ca^{2+} can lead to the occurrence of apoptosis (Jiang et al., 1994).

The release of Ca^{2+} from the endoplasmic reticulum into the cytoplasm has been implicated as a key-signaling

event in many models of apoptosis and it may sensitize mitochondria to trigger apoptotic cell death. In addition, an increasing number of endoplasmic reticulum proteins have been described to influence apoptosis by either interacting with Bcl-2 family members or altering endoplasmic reticulum Ca^{2+} responses. Also, several endoplasmic reticulum proteins are caspase substrates that may regulate the execution phase of apoptosis (Breckenridge, 2003).

Generally, in response to endoplasmic reticulum stress, Bax and Bak undergo conformational changes to cause the release of Ca^{2+} from endoplasmic reticulum lumen into cytoplasm, followed by the activation of calpain. Upon exposure to Ca^{2+} , calpain subunits undergo auto-cleavage, which facilitates activation and ultimately leads to calpain degradation (Goll, 2003). Beside the participation in apoptosis by cleaving either pro-apoptotic and anti-apoptotic proteins based on the nature of stimuli and type of cells involved, calpain has been reported to cleave caspase-4 that is supposed to function in endoplasmic reticulum stress-mediated apoptosis (Hitomi, 2004).

Mitochondrion is an intracellular calcium store. The Ca^{2+} uptake depends on mitochondrial trans-membrane potential. Mitochondrial Ca^{2+} elevation mechanisms include non-specific leakage and pore formation. With the existence of proper stimulus, Ca^{2+} is released from mitochondrion and endoplasmic reticulum. Mitochondrial calcium overload leads to mitochondrial damage, release of cytochrome C and caspase activation, and subsequent apoptosis.

Phloretin can exert significant effect on Ca^{2+} current (Olson et al., 2007). Our data demonstrated when phloretin induced apoptosis of SMMC-7721 cells, cytosolic free Ca^{2+} concentration increased, so that Ca^{2+} homeostasis was disturbed. It indicates appropriate concentration of phloretin has significant effects in inducing apoptosis on SMMC-7721 cells. The result of disturbed calcium homeostasis, taken together with mitochondrial trans-membrane potential decrease, presumably links it with endoplasmic reticulum calcium release.

In conclusion, our results show that phloretin induces apoptosis in hepatoma cells by inhibiting DNA synthesis, reducing mitochondrial membrane potential and interfering calcium homeostasis. These findings may have potential applications in the treatment of liver cancer. The results demonstrate that phloretin might be developed into a new anti-cancer drug.

ACKNOWLEDGEMENTS

The work was supported by the "863" National Major Research Program (2007AA10Z170), and National Key Technology R&D Program (2006BAD13B08, 2007AA10Z170).

Abbreviations: PDT, population doubling time; DMEM, Dulbecco's modified Eagle's medium; DMSO, Dimethyl sulfoxide; MTT, 3-(4, 5-dimethylthiazol-2-yl)-2, 5-diphenyl-2H-tetrazolium bromide; FBS, fetal bovine serum; AO, acridine orange; EB, ethidium bromide; FITC, fluorescein isothiocyanate; PI, propidium iodide; PBS, phosphate buffered saline; FCM, flow cytometer; AIF, apoptosis inducing factor.

REFERENCES

- Adachi T (2008). Fret-based Ca^{2+} measurement in B lymphocyte by flow cytometry and confocal microscopy. *Biochim. Biophys. Res.*, 367: 377-382.
- Alexeyev MF (2009). Is there more to aging than mitochondrial DNA and reactive oxygen species? *FEBS J.*, 276: 5768-5787.
- Armstrong JS (2006). Mitochondrial membrane permeabilization: the sine qua non for cell death. *Bioessays*, 28: 253-260.
- An RB, Park EJ, Jeong GS, Sohn DH, Kim YC (2007). Cytoprotective constituent of *Hoveniae Lignum* on both HepG2 cells and rat primary hepatocytes. *Arch. Pharm. Res.*, 30: 674-677.
- Auner BG, Valenta C, Hadgraft J (2003). Influence of phloretin and 6-ketocholestanol on the skin permeation of sodium-fluorescein. *J. Control. Release.*, 89: 321-328.
- Blazso G, Gabor M (1995). Effects of prostaglandin antagonist phloretin derivatives on mouse ear edema induced with different skin irritants. *Prostaglandins*, 50: 161-168.
- Blobel GA, Orkin SH (1996). Estrogen-induced apoptosis by inhibition of the erythroid transcription factor GATA-1. *Mol. Cell Biol.*, 16: 1687-1694.
- Bouchier-Hayes L, Lartigue L, Newmeyer D (2005). Mitochondria: pharmacological manipulation of cell death. *J. Clin. Invest.*, 115: 2640-2647.
- Breckenridge DG (2003). Caspase cleavage product of BAP31 induces mitochondrial fission through endoplasmic reticulum signals, enhancing cytochrome c release to the cytosol. *J. Cell Biol.*, 160: 115-127.
- Brown JM, Attardi LD (2005). The role of apoptosis in cancer development and treatment response. *Nat. Rev. Cancer.*, 5: 231-237.
- Cadenas E, Davies KJA (2000). Mitochondrial free radical generation, oxidative stress, and aging. *Free Radic. Biol. Med.*, 29: 222-230.
- Cetindere T, Nambiar S, Santourlidis S, Essmann F, Hassan M (2010). Induction of indolamine 2, 3-deoxygenase by death receptor activation contributes to apoptosis of melanoma cells via mitochondrial damage-dependent ROS accumulation. *Cell Signal*, 22: 197-211.
- Chih-Hsiung Wu, Yuan-Soon Ho, Chia-Yi Tsai, Ying-Jan Wang, How Tseng, Po-Li Wei, Chia-Hwa Lee, Ren-Shyan Liu, Shyr-Yi Lin (2009). In vitro and in vivo study of phloretin-induced apoptosis in human liver cancer cells involving inhibition of type II glucose transporter. *Int. J. Cancer.*, 124: 2210-2219.
- Disa N, Bailly C (2005). Drugs targeting mitochondrial functions to control tumor cell growth. *Bilchem. Pharmacol.*, 70: 1-12.
- Frantz DJ, Hughes BG, Nelson DR (2000). Cell cycle arrest and differential gene expression in HT-29 cells exposed to an aqueous garlic extract. *Nutr. Cancer.*, 38: 255-264.
- Goll DE (2003). The calpain system. *Physiol. Rev.*, 83: 731-801.
- Gschwendt M, Horn F, Kittstein W (1984). Calcium and phospholipid-dependent protein kinase activity in mouse epidermis cytosol. Stimulation by complete and incomplete tumor promoters and inhibition by various compounds. *Biochem. Biophys. Res. Commun.*, 124: 63-68.
- Guan WJ, Ma YH, Zhou XY (2005). The establishment of fibroblast cell line and its biological characteristic research in Tai hang black goat. *Review of China. Agric. Sci. Technol.*, 7: 25-33.
- Gu Y, Li H, Miki J, Kim KH, Furusato B, Sesterhenn IA, Chu WS, McLeod DG, Srivastava S, Ewing CM, Isaacs WB, Rhim JS (2006). Phenotypic characterization of telomerase-immortalized primary non-malignant and malignant tumor-derived human prostate epithelial cell lines. *Exp. Cell Res.*, 312: 831-843.
- Hertel C, Terzi E, Hauser N (1997). Inhibition of the electrostatic

- interaction between beta-amyloid peptide and membranes prevents beta-amyloid-induced toxicity. *Proc Natl Acad Sci USA*, 94: 9412-9416.
- He X, Liu RH (2007). Triterpenoids isolated from apple peels have potent antiproliferative activity and may be partially responsible for apple's anticancer activity. *J. Agric. Food Chem.*, 55: 4366-4370.
- Hitomi J (2004). Involvement of caspase-4 in endoplasmic reticulum stress-induced apoptosis and Ab-induced cell death. *J. Cell Biol.*, 165: 1-10.
- Ho YS, Wu CH, Chou HM, Wang YJ, Tseng H, Chen CH, Chen LC, Lee CH, Lin SY (2005). Molecular mechanisms of econazole-induced toxicity on human colon cancer cells: G0/G1 cell cycle arrest and caspase-8 independent apoptotic signaling pathways. *Food Chem. Toxicol.*, 43: 1483-1495.
- Jarvis WD, Turner AJ, Povirk LF, Traylor RS, Grant S (1994). Induction of apoptotic DNA fragmentation and cell death in HL-60 human promyelocytic leukemia cells by pharmacological inhibitors of protein kinase C. *Cancer. Res.*, 54: 1707-1714.
- Jiang S, Chow SC, Nicotera P, Orrenius S (1994). Intracellular Ca²⁺ signals activate apoptosis in thymocytes: Studies using the Ca²⁺-ATPase inhibitor thapsigargin. *Exp Cell Res.*, 212: 84-92.
- Johansson AC, Steen H, Ollinger K, Roberg K (2003). Cathepsin D mediates cytochrome c release and caspase activation in human fibroblast apoptosis induced by staurosporine. *Cell Death and Differentiation*, 10: 1253-1259.
- Jonge PD, Wieringa T, Van Putten JP (1983). Phloretin - an uncoupler and an inhibitor of mitochondrial oxidative phosphorylation. *Biochim. Biophys. Acta*, 722: 219-225.
- Kong D, Nishino N, Shibusawa M, Kusano M (2007). Establishment and characterization of human pancreatic adenocarcinoma cell line in tissue culture and the nude mouse. *Tissue Cell.*, 39: 217-223.
- Kroemer G, El-Deiry WS, Golstein P, Peter ME, Vaux D, Vandenberghe P, Zhivotovsky B, Blagosklonny MV, Malorni W, Knight RA, Piacentini M, Nagata S, Melino G (2005). Classification of cell death: Recommendations of the nomenclature committee on cell death. *Cell Death. Differentiation*, 12: 1463-1467.
- Liu X, Zou H, Slaughter C, Wang X (1997). DFF, a heterodimeric protein that functions downstream of caspase-3 to trigger DNA fragmentation during apoptosis. *Cell*, 89: 175-184.
- Lucken-Ardjomande S, Montessuit S, Martinou JC (2005). Changes in the outer mitochondrial membranes during apoptosis. *J. Soc. Biol.*, 199: 207-210.
- Mohamad N, Gutierrez A, Nunez M (2005). Mitochondrial apoptotic pathways. *Biocell*, 29: 149-161.
- Moley KH, Mueckler MM (2005). Glucose transport and apoptosis. *Apoptosis*, 5: 99-105.
- Moridani MY, Galati GO, Brien PJ (2002). Comparative quantitative structure toxicity relationships for flavonoids evaluated in isolated rat hepatocytes and HeLa tumor cells. *Chem. Biol. Interact.*, 139: 251-264.
- Nakamura N, Wada Y (2000). Properties of DNA fragmentation activity generated by ATP depletion. *Cell Death Differ.*, 7: 477-484.
- Nelson JA, Falk RE (1993). The efficacy of phloridzin and phloretin on tumor cell growth. *Anticancer. Res.*, 13: 2287-2292.
- Olson ML, Kargacin ME, Ward CA (2007). Effects of phloretin on Ca²⁺ handling, the action potential, and ion currents in rat ventricular manocytes. *Pharmacol. Exp. Ther.*, 321: 921-929.
- Oresajo C (2008). Protective effects of a topical antioxidant mixture containing vitamin C, ferulic acid, and phloretin against ultraviolet-induced photodamage in human skin. *J. Cosmet. Dermatol.*, 7: 290-297.
- Raja M, Tyagi NK, Kinne RK (2003). Phlorizin recognition in a C-terminal fragment of SGLT1 studied by tryptophan scanning and affinity labeling. *Biol. Chem.*, 278: 49154-49163.
- Richter C, Schweizer M, Cossarizza A, Franceschi C (1996). Control of apoptosis by the cellular ATP level. *FEBS Lett.*, 378: 107-110.
- Siegers CP, Steffen B, Robke A (1999). The effects of garlic preparations against human tumor cell proliferation. *Phyto-medicine*, 6: 7-11.
- So Y,P, Eun Ji K, Hyun-Kyung S (2006). Induction of apoptosis by phloretin in HT229 human coloncancer cells. *FASEB J.* A, 20: 5681.
- Yang KC, Wu CC, Wu CH, Chen JH, Chu CH, Chen CH, Chou YH, Wang YJ, Lee WS, Tseng H, Lin SY, Lee CH (2006). Involvement of proapoptotic Bcl-2 family members in terbinafine-induced mitochondrial dysfunction and apoptosis in HL60 cells. *Food Chem. Toxicol.*, 44: 214-226.
- Yoon H, Liu RH (2007). Effect of selected phytochemicals and apple extracts on NF-kappaB activation in human breast cancer MCF-7 cells. *J. Agric. Food Chem.*, 55: 3167-3173.
- Zhang HT, Feng ZL, Wu J, Wang YJ, Guo X, Liang NC, Zhu ZY, Ma JQ (2007). Sodium butyrate-induced death-associated protein kinase expression promote Raji cell morphological change and apoptosis by reducing FAK protein levels. *Acta. Pharmacol. Sin.*, 28: 1783-1790.
- Zhang HT, Wu J, Zhang HF, Zhu QF (2006). Efflux of potassium ion is an important reason of HL-60 cells apoptosis induced by Tachyplesin. *Acta. Pharmacol. Sin.*, 27: 1367-1374.
- Zhou XM, Ma YH, Guan WJ (2004). Establishment and identification of Debao pony ear marginal tissue fibroblast cell line. *Asian-Australian. J. Ani. Sci.*, 17: 1338-1343.